Macromolecules

ARTICLE

pubs.acs.org/Macromolecules

Hydration Mediation in Supported Aqueous-Phase Catalysis for Atom Transfer Radical Polymerization

Ravi Aggarwal[†] and Durairaj Baskaran*

Department of Chemistry, University of Tennessee, Knoxville, Tennessee 37996, United States

Supporting Information

ABSTRACT: Hydrated sodium montmorillonite (Na-clay) and silica gel are used as solid supports for atom transfer radical polymerization (ATRP) of benzyl methacrylate and methyl methacrylate. The catalyst complexes of $CuBr_2$ and CuBr with *N,N,N′,N′,N″*-pentamethyldiethylenetriamine, which are physically adsorbed on Na-clay and silica gel, are efficiently retained by the solid supports via small amounts of hydration. The supported aqueous-phase catalysis (SAPC) over Na-clay and silica produces catalyst-free polymers for activator generated electron transfer ATRP and conventional ATRP processes. The kinetics for the catalyst supported Na-clay and silica systems show that the polymerization proceeded only in the presence of hydrated catalyst support and ceased when the polymerization solution was separated from the hydrated catalyst support. In the case of Na-clay SAPC, the polymerization follows a linear first-order time−conversion plot and produces polymers with moderately narrow molecular weight distribution (MWD, $M_w/M_n \leq 1.30$). However, for silica SAPC the first-order time−conversion plot is curved, indicating that the polymerization proceeds with termination and polymers exhibited broad MWD ($M_w/M_n > 1.50$). The poor performance of silica SAPC is attributed to the inefficient mobility of the catalyst and the nature of hydrogen bonding of the water molecules on its surface. The bilogarithmic plot of apparent rate constant k_{app} vs $[I]_0$ in SAPC for ATRP indicates a zero order, suggesting that the polymerization is independent of the bulk initiator concentration, and the propagation is confined to the hydrated interface between the solid support and the organic phase.

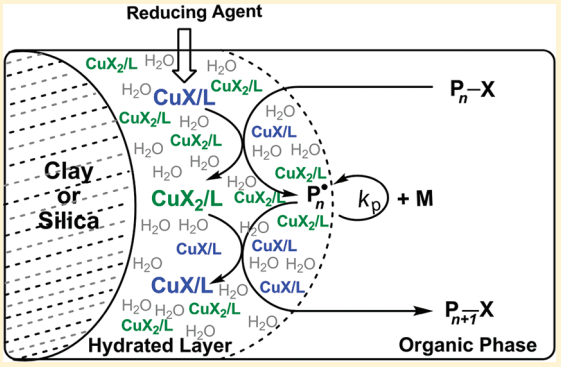

INTRODUCTION

Metal-catalyzed atom transfer radical polymerization (ATRP) is a versatile "living"/controlled polymerization technique for the synthesis of tailor-made vinyl polymers with narrow molecular weight distribution (MWD, M_w/M_n).[1−3] Numerous catalyst systems based on Cu, Ru, Ni, and Rh have been developed and applied successfully for the ATRP of styrenic, acrylic, and methacrylic monomers.[2,4−9] The process requires the use of high concentration of metal catalyst to maintain a favorable redox equilibrium, and thus, the postpurification of polymer from the catalyst contamination is essential. This severely limits the viability of ATRP for commercial polymer production.[10] Several postpurification methods for the removal of copper catalyst have been reported.[10−16] They include passing the polymer solution through a column containing adsorbents such as alumina or silica gel, repeated solvent washing, extraction, and selective precipitation.[10] In addition, ion-exchange and Janda Jel resins have also been used to remove the catalyst from ATRP solution.[16,17] These methods are time-demanding and costly. Therefore, it is necessary to develop a new method which reduces the amount of catalyst in the ATRP process or can allow the catalyst be recovered for reuse.

Matyjaszewski and co-workers have developed new initiating systems such as the activator generated or regenerated electron transfer (AGET or ARGET) ATRPs mainly focused to reduce the catalyst concentration.[18−23] In a typical AGET system, a transition metal catalyst in its higher oxidation state such as Cu^{II} complex is used, and the active species of Cu^{I} complex is generated via *in situ* reduction using reducing agent (Sn^{II} 2-ethylhexanoate or ascorbic acid). In the ARGET ATRP system, an excess of reducing agent is used which allows for a substantial reduction of the catalyst concentration in the polymerization. However, an excessive amount can cause continuous reduction of Cu^{II} which leads to an inefficient deactivation ($k_{act} \gg k_{deact}$) and affects the control of the polymerization producing polymers with broad MWD.[20] Still, the concentration of residual metal catalyst in the polymer obtained from these processes is not sufficiently low for it to be directly used in commercial application.[10,24]

A potential solution to this problem is to support the catalyst on a solid support that can be separated easily from the polymer solution and efficiently recycled. The strategies that have been employed with limited success include the use of supported catalyst systems based on silica, ion-exchange resins, cross-linked

Received: August 26, 2011
Revised: September 27, 2011
Published: October 25, 2011

polystyrene beads, reversible supported and hybrid catalysts, and soluble biphasic and polymer anchored catalyst systems.[16,17,25−32] The supported catalyst systems are broadly classified into three categories: (a) covalent, (b) physisorbed, and (c) biphasic. The major problem associated with the covalent strategies is the limited mobility of the catalyst, thereby making its accessibility to the diffusing radicals in the solution extremely difficult. Many research groups, Matyjaszewski, Haddleton, Jones, and Zhu, and their co-workers, have performed heterogeneous ATRP using covalently supported silica catalyst systems.[25,29,31,33,34] The polymers exhibited broad MWD with poor initiator efficiency. Matyjaszewski and Zhu and their co-workers attributed the poor efficiency to diffusion-controlled deactivation process.[25,35] The problem in the supported heterogeneous ATRP is not entirely due to the polymer diffusion limitation, but an inefficient deactivation of the radicals due to geographical isolation of the catalyst complexes at the surface. Moreover, every recycling attempts showed a further decrease in efficiency and more catalyst leaching. On the other hand, the physisorption method using silica as a support suffers from extensive leaching problem.[25,26,30,31,36] Although biphasic and recoverable catalysts are relatively more efficient than the solid supported catalysts, their complex preparation and recovery procedures are tedious and limit their applicability.[14,37,38]

An ideal solid supported catalyst system should have characteristics of both the heterogeneous (for easy recovery/reuse) and the homogeneous (for effective control of the polymerization) systems. In the case of ATRP, the support should provide an easy accessibility to lower and higher oxidation state transition metal complexes for activation of dormant and deactivation of radical intermediates in close proximity to circumvent diffusion-related problems and to maintain a favorable redox equilibrium. Unfortunately, almost all the catalyst immobilization strategies suffer significantly from insufficient catalyst mobility and produce polymers with a broad MWD due to uncontrolled chain growth and termination, except the strategies that have some amount of catalyst leaching into the solution.[10,30,35,36] We have recently exploited hydration as a means to mobilize the catalyst complexes on clay and recycled the supported catalyst over 21 times efficiently.[39−42] Hydration played a critical role in retaining the catalyst on the support and provided the control over the polymerization.

In this report, we examine supported aqueous-phase catalysis (SAPC) of two different inorganic supports such as clay and silica gel for ATRP. We show that the control of ATRP is primarily dependent on the surface arrangement of water molecules at the hydrated interface of the support. We compare the efficiencies of Na-clay and silica gel SAPC systems for ATRP process via kinetics and mechanistic studies. Efficacy of SAPC for ATRP of methyl methacrylate (MMA) and benzyl methacrylate (BnMA) to produce controlled molecular weight polymers without catalyst contamination using hydrated clay and silica is discussed in terms of catalyst mobility related to water diffusivity on the support surface.

EXPERIMENTAL SECTION

Materials. The reagents CuBr, $CuBr_2$, *N,N,N′,N′,N″*-pentamethyldiethylenetriamine (PMDETA), toluene, BnMA, MMA, silica gel (230−400 mesh), basic aluminum oxide, sodium ascorbate (NaAsc), ethyl 2-bromoisobutyrate (EBriB), dry anisole, *n*-hexane, tetrahydrofuran (THF, HPLC grade), calcium hydride, and methanol were purchased from Aldrich. PMDETA, toluene, and dry anisole were used after degassing with ultrapure N_2. EBriB was distilled over CaH_2 under high vacuum and stored at −20 °C under a N_2 atmosphere. Monomers, BnMA and MMA, were passed through a basic alumina column in order to remove the inhibitor and were stored at −20 °C under N_2. Sodium montmorillonite (Closite Na^+/Na-clay) was obtained from Southern Clay Products and used as received. The other reagents were used as received without any further purification. Deionized (DI) water was used to prepare an aqueous solution of NaAsc.

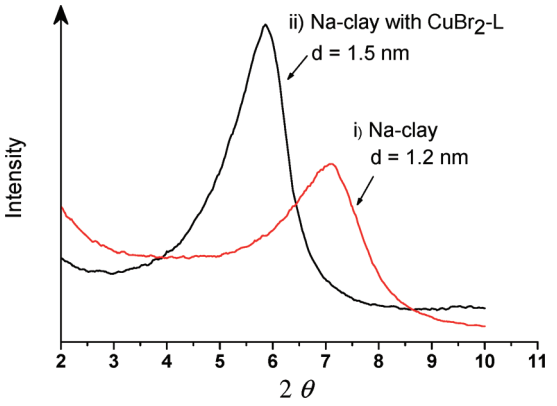

Figure 1. XRD of Na-clay and $CuBr_2$/PMDETA intercalated Na-clay.

Preparation of $CuBr_2$/PMDETA Intercalated Na-Clay. In a 250 mL round-bottom flask containing a magnetic stir bar, 0.55 g (2.46 mmol) of $Cu^{II}Br_2$ was dissolved in 100 mL of methanol. To this, an equimolar amount of ligand, PMDETA (0.427 g, 2.46 mmol), was added dropwise to form a homogeneous catalyst complex solution. Thereafter, 5.5 g of Na-clay (Cu^{II}/Na-clay = 10 wt %, $[Cu^{II}]/[Na^+]_{clay}$ = 0.5) was added and stirred for 30 min. The methanol was removed using a rotary evaporator, and the residue, a blue Na-clay supported catalyst, was dried under high vacuum for 2−3 h at room temperature. The blue Na-clay supported catalyst was characterized using X-ray diffraction (XRD) (Figure 1). XRD *d*-spacing: Na-clay = 1.2 nm and Na-clay/$CuBr_2$−PMDETA = 1.5 nm.

Preparation of $CuBr_2$/PMDETA Loaded Silica Supported Catalyst. In a 250 mL round-bottom flask, 0.550 g of $Cu^{II}Br_2$ (2.46 mmol) was charged with 100 mL of methanol. An equimolar amount of ligand, PMDETA, (0.427 g, 2.46 mmol), was added to form a homogeneous catalyst complex solution. To this, 5.50 g of silica gel (Cu^{II}/silica = 0.1) was added and stirred for 30 min. The methanol was removed using a rotary evaporator, and the residue, a blue silica supported catalyst, was dried under high vacuum for 1 h at room temperature (Figure 2). The intensity of the blue color of the $CuBr_2$/PMDETA physisorbed silica varied depending on the concentration of the catalyst loaded on the surface of the support.

Kinetics of AGET ATRP of BnMA Using Na-Clay Supported $CuBr_2$/PMDETA. The supported catalyst was dried at 60 °C for 1 h under vacuum prior to use. For a typical kinetics of the BnMA polymerization 272 mg of clay/$CuBr_2$−PMDETA (Cu^{II}/Na-clay = 10 wt %) was taken in a Schlenk tube and degassed using vacuum−nitrogen cycles twice. Thereafter, anisole (1:1 v/v), BnMA (2.95 mol/L), and NaAsc (2.2 mg, 1.12×10^{-5} mol, $[NaAsc]_0/[I]_0 = 0.17$) in 41 μL of DI water (H_2O/clay = 15 wt %) were added for the polymerization in the sequence as described. The blue color of the clay catalyst slowly changed to bluish-green, indicating the reduction of $Cu^{II}Br_2$ to $Cu^{I}Br$ in the hydrated layers of the clay. Polymerization was initiated using EBriB (4.1×10^{-3} mol/L) as an initiator at 40 °C. A small amount (~0.2 mL) of supernatant solution was withdrawn at regular intervals for the determination of monomer conversion using ^{1}H NMR and number-average molecular weight (M_n) using size exclusion chromatography (SEC) coupled with light scattering detectors (SEC-LS). Conversion = 53%, $M_{n,LS}$ = 131 000 g/mol, M_w/M_n = 1.26, initiator

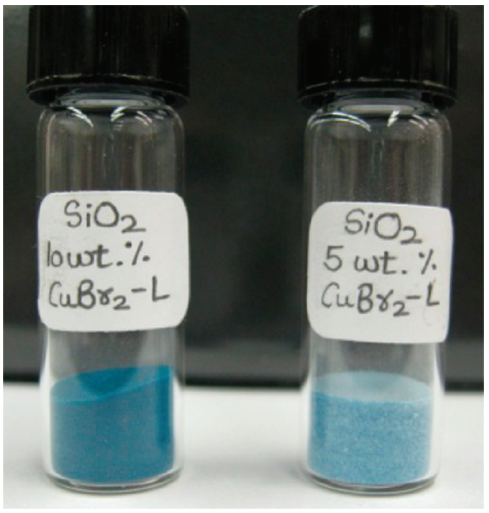

Figure 2. Vials containing catalyst complex ($CuBr_2$/PMDETA) physically adsorbed on silica gel Cu^{II}/silica = 10 and 5 wt %.

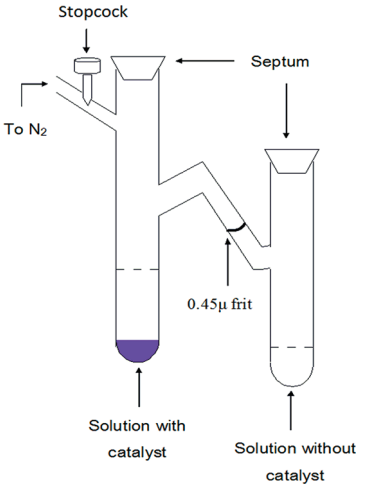

Figure 3. Diagram of custom-built glass apparatus for split-kinetics experiments.

efficiency, $f\,(M_{n,th}/M_{n,LS})$ = 0.52 where $M_{n,LS}$ is the molecular weight determined from SEC-LS and $M_{n,th}$ is the theoretical molecular weight calculated based on the feed ratio of grams of monomer/moles of initiator.

Split-Kinetics of BnMA Polymerization Using Na-Clay Supported $CuBr_2$/PMDETA Catalyst Complex. The split-kinetics experiment was performed using a specially designed glass apparatus (Figure 3). The glass reactor had 0.45 μm frit filter disk to avoid passing of any supported catalyst while filtering the polymerization solution containing the supported catalyst.

The experiment was conducted with 272 mg of Na-clay loaded 10 wt % $CuBr_2$/PMDETA catalyst in the presence of H_2O/clay = 15 wt % and $[NaAsc]_0/[I]_0$ = 0.17 in anisole at 40 °C with EBriB as an initiator (3.3×10^{-3} mol/L). A portion of the solution was filtered through a 0.45 μm frit at an appropriate time into another part of the apparatus, and aliquots (~0.2 mL) were withdrawn from both the reaction tubes at regular intervals for estimation of monomer conversion, molecular weight, and MWD. The final conversion, $M_{n,LS}$, and MWD of the PBnMA were as follows: conversion = 49%, $M_{n,LS}$ = 142 300 g/mol, M_w/M_n = 1.24, $f\,(M_{n,th}/M_{n,LS})$ = 0.54.

ATRP of MMA and BnMA Using Silica Supported CuBr/PMDETA Catalyst Complex. ATRP of MMA (4.68 mol/L) was performed under N_2 in a dry Schlenk tube. In a typical polymerization, 0.5 g of silica and CuBr (25 mg, 1.75×10^{-4} mol, Cu^I/silica = 5 wt %) was taken in a Schlenk tube and was tightly sealed with a rubber septum. Oxygen was removed from the tube by applying vacuum and filling with nitrogen. This procedure was repeated 2−3 times. To this, 5 mL of dry anisole was added followed by the addition of 36 μL of PMDETA (1.75×10^{-4} mol). The mixture was stirred for 15 min, and slowly the solution became faint green in color, indicating a substantial amount of leached catalyst complex in the solution. Then, 5 mL of MMA (4.68 mol/L, 1.77×10^{-2} mol) was added under N_2, and the reaction mixture was stirred for 10 min. Thereafter, 150 μL of DI H_2O (H_2O/silica = 30 wt %) was added in a dropwise manner under constant stirring. The immiscible water droplets slowly disappeared through gradual hydration of silica. The heterogeneous solution was stirred for 1 h. The green color of the silica adsorbed catalyst slowly changed to blue, and the supernatant solution containing monomer became colorless, indicating a complete localization of the catalyst within the hydrated regions of the silica. The reactor was placed in an oil bath maintained at 60 °C. Then, the initiator, BrEiB (1.75×10^{-4} mol, 1.75×10^{-2} mol/L) was added via a gastight syringe to commence the polymerization. The supernatant monomer solution remained colorless during the polymerization. After 4 h, the reaction tube was opened to air to quench the reaction. The polymerization solution was diluted with ~10 mL of toluene and stirred for 30 min in air. The polymer solution containing silica loaded catalyst was filtered using 0.45 μm Teflon membrane. The polymer present in the colorless filtrate was recovered by precipitation in excess of *n*-hexane. The polymer was dried under high vacuum conditions at room temperature for 12 h. The monomer conversion was calculated on the basis of gravimetric yield. The dried polymer was analyzed using SEC calibrated against poly(methyl methcarylate) (PMMA) standards for the determination of molecular weight and MWD. Conversion = 38%, $M_{n,SEC}$ = 16 900 g/mol, M_w/M_n = 1.66, $f\,(M_{n,th}/M_{n,SEC})$ = 0.61.

A typical polymerization of BnMA (2.95 mol/L) was performed in a similar manner using silica (300 mg) supported CuBr/PMDETA (Cu^I/silica = 5 wt %) using H_2O (H_2O/silica = 23.3 wt %) and EBriB (5.3×10^{-3} mol/L) as initiator in anisole (1:1 v/v) at 25 °C. The molecular weight was calculated using SEC-LS and MWD using SEC based on polystyrene (PS) standards. Conversion = 24.0%, $M_{n,LS}$ = 88 000 g/mol, M_w/M_n = 1.52, $f\,(M_{n,th}/M_{n,LS})$ = 0.20.

The split-kinetics experiment of BnMA (2.95 mol/L) was conducted in a custom-built glass apparatus (Figure 3) in a same way as described previously for Na-clay supported catalyst system using 0.5 g of silica supported CuBr/PMDETA (Cu^I/silica = 5 wt %) in anisole at 25 °C with H_2O (H_2O/silica = 20 wt %) and EBriB (7.5×10^{-3} mol/L) as initiator. A small amount of sample (~0.2 mL) was withdrawn at regular intervals from the solution with and without catalyst to monitor the growth of the polymerization in both the reactors. The monomer conversions were calculated using ^{1}H NMR, and molecular weights were determined using SEC coupled with light scattering. The filtered solution was investigated for the presence of residual copper catalyst by UV−vis spectroscopy. With catalyst: conversion = 59.7%, $M_{n,LS}$ = 66 500 g/mol, M_w/M_n = 1.61, $f\,(M_{n,th}/M_{n,LS})$ = 0.62.

AGET ATRP of BnMA Using Silica Supported $CuBr_2$/PMDETA Catalyst Complex. A typical AGET ATRP of BnMA (2.95 mol/L) was performed using 600 mg of silica supported $CuBr_2$/PMDETA (Cu^{II}/silica = 5 wt %) in anisole (1:1 v/v) at 25 °C in the presence of H_2O (H_2O/silica = 17 wt %) and NaAsc as a reducing agent ([NaAsc]/[I] = 0.2) in a similar manner as described previously for the Na-clay supported catalyst system. Conversion = 59.7%, $M_{n,LS}$ = 93 600 g/mol, M_w/M_n = 1.61, $f\,(M_{n,th}/M_{n,LS})$ = 0.49.

Characterization. ^{1}H NMR spectra were recorded using Bruker AC250 spectrometer at 250 MHz. The samples were prepared in $CDCl_3$

Scheme 1. AGET ATRP of BnMA Using Hydrated Na-Clay and Hydrated Silica Supported Catalyst Systems in Anisole at Ambient Temperature

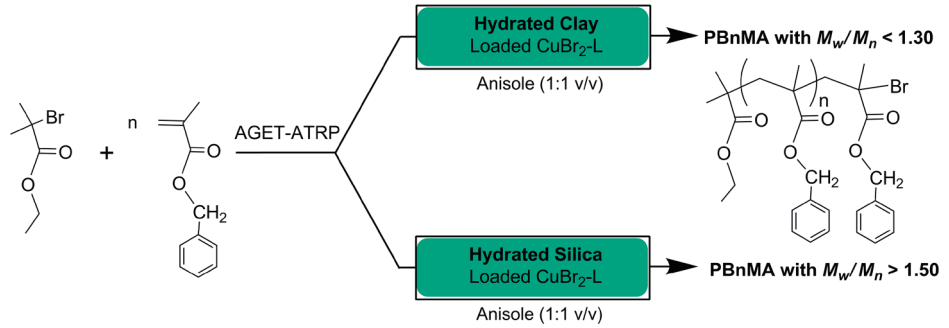

containing 1% TMS as an internal reference. Monomer conversions were calculated from the intensity ratio of the $-OCH_3$ signal (δ = 3.76 ppm) corresponding to anisole and a double-bond proton signal (δ = 6.15 ppm) of the monomer.

M_n and MWD were determined using SEC equipped with Knauer's K-501 HPLC pump, K-2301 RI detector, and K-2501 UV detector. The columns used were two 60 cm PSS SDV-gel: 1 × 10 μm/100 Å, 1 × 5 μm/linear: 10^2-10^6 Å. THF was used as an eluent at a flow rate of 1.0 mL/min, and the calibration of SEC was performed using PS standards obtained from Pressure Chemicals (Pittsburgh, PA).

Refractive index increment (dn/dc) was determined using Brice Phoenix BP-2000-V differential refractometer at the wavelength of 690 nm. The value of dn/dc (0.151 mL/g) was determined using five different concentrations (1, 5, 10, 15, and 20 mg/mL) of PBnMA in THF. Absolute molecular weights were measured using light scattering ($M_{n,LS}$) instrument comprising of Wyatt DAWN EOS (enhanced optical system) multiangle laser light scattering detector (MALLS) and an Optilab DSP interferometric refractometer. The following PSS SDV-gel columns were used: guard (8 × 50 mm), 10^6 Å (8 × 300 mm), 10^5 Å (8 × 300 mm), 10^3 Å (8 × 300 mm), and 500 Å (8 × 300 mm). THF was used as a solvent at the flow rate of 1.0 mL/min. Linear PSt standards from Pressure Chemicals (Pittsburgh, PA) were used to calibrate the instrument.

XRD experiments were performed on Philips X'Pert diffractometer equipped with copper target and a diffracted beam monochromator (Cu Kα radiation at λ = 1.5406 Å) at 45 mA and 40 kV. Evolution 600 UV−vis spectrometer was used to determine the amount of copper present in the polymer solutions and a known concentration of $CuBr_2$−PMDETA solution in DMSO was used for the calibration (λ_{max} = 716 nm). The FT-IR spectrum was recorded using Varian 4100 (Excalibur series). The samples were prepared using the KBr pellet method. Differential scanning calorimetry (DSC) was performed using a TA Instruments DSC Q1000 under nitrogen with a heating rate of 10 °C/min.

RESULTS AND DISCUSSION

We have shown previously that the Na-clay supported AGET ATRP of BnMA proceeds efficiently and produces catalyst-free polymer in the presence of a small amount of water.[39] The hydration played a key role in retaining the catalyst on the surface of clay and was attributed for facilitating the catalyst mobility for rapid deactivation of active radicals. In order to understand the influence of hydration and to examine the applicability of a similar mechanism for silica gel support, which has been studied extensively in the literature, we performed polymerizations of BnMA and MMA using hydrated Na-clay and silica gel as supports for comparison (Scheme 1). Several batch polymerizations were carried out in anisole using hydrated Na-clay and silica supported with $CuBr_2$/PMDETA and CuBr/PMDETA complexes, respectively. The $CuBr_2$/PMDETA complex was loaded with Na-clay by kneading for AGET ATRP, and the CuBr/PMDETA complex was loaded with silica by simply mixing under nitrogen in the presence of anisole for ATRP. In the case of Na-clay supported Cu^{II} catalyst system, the active Cu^{I} complex was generated *in situ* via addition of aqueous solution of reducing agent, NaAsc. The blue color of the catalyst on Na-clay changed to bluish-green upon addition of a known quantity of aqueous NaAsc solution, indicating the generation of Cu^{I} on the surface of clay. Once the active catalyst was generated, the initiator (EBriB) was added to commence the polymerization (Scheme 1).

The optimum conditions of hydration (10 wt % ≤ H_2O/support ≤ 30 wt %) and reducing agent (0.15 ≤ [NaAsc]/[I] ≤ 0.23) were used for the polymerization BnMA. The polymerization proceeded smoothly in the presence of hydrated Na-clay support containing both Cu^{I} and Cu^{II} catalyst complexes and produced catalyst-free PBnMA in solution with moderate MWD (M_w/M_n ≤ 1.31; Table 1, runs 1 and 2, Figure 4a). The supernatant organic phase (anisole) containing the initiator/dormant chain and the monomer remained colorless throughout the polymerization. The supernatant solution taken during the polymerization showed insignificant UV−vis absorbance at λ_{max} 760 nm, indicating an absence of copper complexes in the solution (Figure 6ii).

In the case of silica gel supported catalyst system, ATRP of MMA and BnMA was performed using hydrated silica supported CuBr-PMDETA catalyst in order to overcome the leaching problem reported in previous studies.[36] After the addition of monomer (BnMA or MMA), solvent, and PMDETA to the solid mixture consisting of silica gel and CuBr, the color of the silica gel turned green and the anisole solution became slightly green, too (Figure 5i). The green color of the anisole indicates the presence of leached catalyst complexes from the silica. Upon hydration (H_2O/silica gel = 17−30 wt %) the leached catalyst in anisole slowly got adsorbed onto the silica. Also, the green color of the catalyst adsorbed silica turned blue and the anisole solution became colorless (Figure 5ii), indicating a complete retention of the catalyst complex on the surface of silica via hydration.

ATRP of MMA (4.68 mol/L) using hydrated (H_2O/silica = 30 wt %) silica supported CuBr-PMDETA (Cu^{I}/silica gel = 5 wt %) at 60 °C was initiated through the addition of EBriB in known quantity (Table 1, runs 3 and 4). The polymerization was

Table 1. SAPC for ATRP of BnMA at 25 °C and MMA at 60 °C Using Na-Clay and Silica Supported Copper−PMDETA Complexes in the Presence of Water Using NaAsc as Reducing Agent and EBriB (I) as Initiator[a]

run	clay or silica (mg)	$[I] \times 10^3$ (mol/L)	M/I/Cu^x/L[b]	H_2O/support (wt %)[c]	[NaAsc]/[I]	conv[d] (%)	$M_{n,th}$[e] $\times 10^{-3}$ (g/mol)	$M_{n,SEC}$[f] $\times 10^{-3}$ (g/mol)	$M_{n,LS}$[g] $\times 10^{-3}$ (g/mol)	M_w/M_n[f]
	clay-$CuBr_2$-L/BnMA									
1	344	10.2	289/1/2/2	14.0	0.15	33.6	17.1	42.5	66.3	1.31
2	272	5.5	536/1/2/2	17.0	0.15	55.0	51.7	63.5	99.1	1.26
	silica-CuBr-L/MMA									
3	500	17.4	269/1/1/1	30.0	0	38.0	10.2	16.9	—[k]	1.66
4[h]	500	17.4	269/1/1/1	30.0	0	36.7	9.9	16.1	—[k]	1.64
	silica-CuBr-L/BnMA									
5	300	5.3	450/1/1/2	23.3	0	24.0	19.1	56.4	88.0	1.52
6[i]	500	7.5	393/1/1/2	20.0	0	59.7	41.4	42.6	66.5	1.75
7[j]	500	7.5	393/1/1/2	17.0	0	40.0	27.7	17.9	279.2	2.20
	silica-$CuBr_2$-L/BnMA									
8	600	6.8	434/1/2/2	17.0	0.20	59.7	45.6	60.0	93.6	1.61
9	272	6.6	357/1/1/1	18.0	0.23	37.0	23.6	90.7	141.5	1.53

[a] Reaction condition: Cu^{II}/Na-clay = 10 wt %, (Cu^I or Cu^{II})/silica = 5 wt %, [BnMA] = 2.95 mol/L in anisole (1:1 v/v), [MMA] = 4.68 mol/L in toluene (1:1 v/v). [b] Mole ratio of M = MMA or BnMA, I = EBriB, Cu^x = CuBr or $CuBr_2$ where x is the oxidation number, and L = PMDETA. [c] wt % of hydration on the support via drop by drop addition of water. [d] Conversion was calculated gravimetrically. [e] $M_{n,th}$ = (grams of monomer/mol of initiator) × conv. [f] Molecular weights and M_w/M_nwere obtained using SEC calibrated against PS standards. [g] Molecular weights obtained using SEC-MALLS using dn/dc of 0.151 mL/g. [h] Polymerization performed in the presence of 0.25 mol % $CuBr_2$ along with CuBr. [i] Split-kinetics experiment. [j] Nanosilica (MCM-41) supported catalyst was used for the polymerization. [k] Not determined.

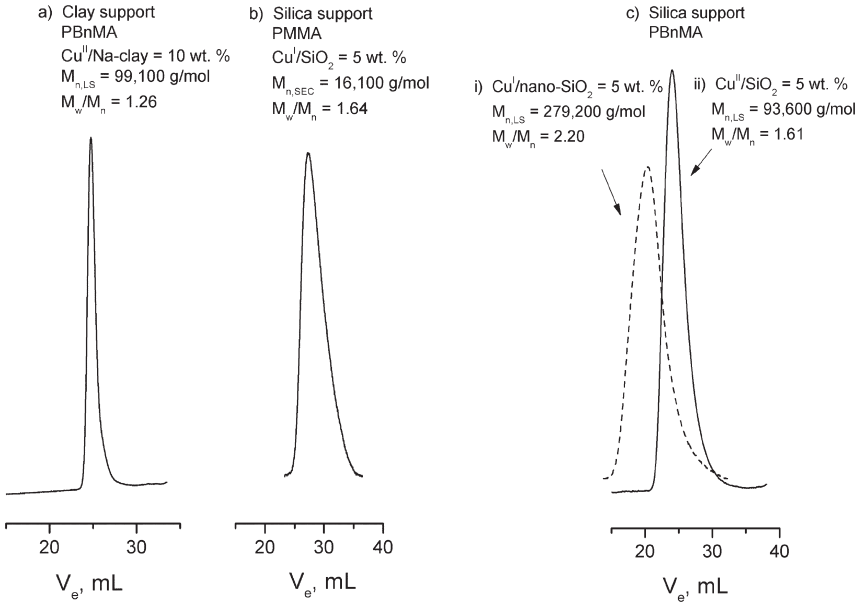

Figure 4. SEC-RI traces of polymers synthesized using hydrated Na-clay and silica supported catalyst systems: (a) PBnMA synthesized using hydrated Na-clay supported $CuBr_2$/PMDETA (Table 1, run 2); (b) PMMA synthesized using hydrated silica supported CuBr/PMDETA with 0.25 mol % $CuBr_2$/PMDETA (Table 1, run 4); (c) PBnMAs synthesized using hydrated nanosilica supported CuBr/PMDETA (i) (Table 1, run 7) and using hydrated silica supported $CuBr_2$/PMDETA (ii) (Table 1, run 8).

terminated after 4 h by exposing the reaction mixture to air. The colorless polymerization solution was filtered and precipitated in *n*-hexane to obtain poly(methyl methacrylate) (PMMA) without any visible traces of residual metal content. The dried PMMA was dissolved in DMSO and analyzed using UV−vis spectroscopy. There was no absorbance at λ_{max} = 716 nm for the PMMA solution in DMSO, further confirming the absence of residual catalyst in the polymer (Figure 6iii).

Unlike other reported silica supported ATRP systems, the hydrated silica support successfully retained the catalyst on the surface. On the other hand, the polymer obtained from hydrated silica catalyst system produced broad MWD ($M_w/M_n \geq 1.52$), which contradicts the polymerization behavior observed in the hydrated Na-clay which gave polymers with narrow MWD ($M_w/M_n \leq 1.31$). More importantly, the experimental molecular weight obtained based on PMMA standards was higher than

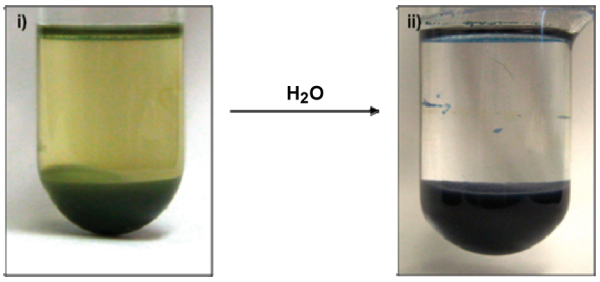

Figure 5. Silica gel supported CuBr/PMDETA catalyst in the solution of monomer and anisole (1:1 v/v): (i) before addition of H_2O; (ii) after addition of H_2O (30 wt %).

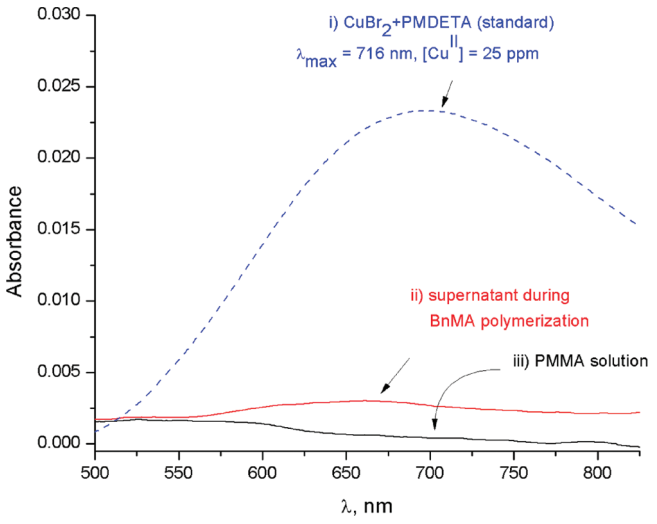

Figure 6. UV−vis absorbance of (i) standard solution of $CuBr_2$−PMDETA for comparison (25 ppm in DMSO), (ii) supernatant during BnMA polymerization over clay supported catalyst, and (iii) PMMA solution in DMSO synthesized using silica supported catalyst.

the theoretical molecular weights calculated from the feed ratio of MMA and initiator (Table 1, run 3). Even with the addition of deactivator ($[Cu^{II}]/[Cu^{I}]$ = 0.25) at the beginning of the polymerization, no improvement in the M_w/M_n of PMMA was observed (Table 1, run 4, and Figure 4b).

Similarly, ATRP of BnMA carried out using silica loaded with 5 wt % CuBr-PMDETA in the presence of water at 25 °C also produced PBnMA with broad MWD (Table 1, runs 5−7). In an effort to increase the surface area of the silica support, hydrated nanosilica/mesoporous silica (Cu^{I}/nanosilica = 5 wt %) was used as a support for the polymerization. However, the catalyst supported on mesoporous silica, which had smaller particle size (~3 nm) and greater surface area (~1000 m^2/g) also produced poorly controlled PBnMA with even broader MWD (M_w/M_n = 2.2; Table 1, run 7, and Figure 4c-i). Obviously, a large surface area of nanosilica provides enhanced interaction of dormant chains that increases the concentration of radicals and thereby side reactions.

The broad MWD of polymers indicates that the deactivation of the radicals is inefficiently occurring at the hydrated silica surface. In an effort to increase the deactivation efficiency, we used higher concentration of deactivator by loading the silica gel with $CuBr_2$/L and attempted AGET ATRP. The AGET ATRP of BnMA was performed over hydrated silica supported $CuBr_2$/PMDETA catalyst (Cu^{II}/silica = 5 wt %) using NaAsc as a reducing agent and EBriB as initiator in anisole at 25 °C (Scheme 1). Surprisingly, the PBnMAs formed in the presence of excess Cu^{II} on the silica support also exhibited broad MWDs in the range 1.53−1.61 (Table 1, runs 8 and 9, Figure 4c-ii). This confirms the availability of catalyst for the deactivation is somehow restricted in the hydrated silica interface. Nevertheless, we were able to effectively contain the catalyst on the silica surface through hydration and prevent catalyst leaching into the organic phase. It should be mentioned that in the previously reported silica supported ATRP systems a small amount of catalyst complex always leaches into the solvent to initiate concurrent polymerization in solution. In fact, it is widely believed that a small amount of leached catalyst is a prerequisite to obtain polymers with narrow MWD in supported ATRP.[43] The hydrated silica supported system described herein showed that the polymerization was confined to the hydrated regions in silica gel similar to Na-clay system. However, the polymers with broad polydispersity indices ($M_w/M_n \geq 1.52$) suggest that even with excess of deactivator ($CuBr_2$/L), the hydrated silica supported catalyst system suffers from slow deactivation.

It is important to note that the hydrated clay catalyst system produced PBnMAs with moderately narrow MWD ($M_w/M_n \leq 1.30$) under the similar conditions. It appears that the availability of the catalyst on the hydrated surface is drastically different in clay and silica. Thus, the actual site of activation/deactivation and the overall influence of hydration mediation in SAPC for ATRP in these supported catalyst systems need to be examined.

Determination of the Location of Catalyst. It was observed during the polymerization in Na-clay and silica supported catalyst systems the supernatant solution was colorless with no UV−vis absorbance at 760 nm, indicating the propagation is occurring at the surface of the supports. In order to confirm the location of the catalyst in Na-clay and silica supported polymerizations, split-kinetics experiment was performed as described by Faucher and Zhu.[36] A small amount of sample (~0.2 mL) was withdrawn at regular intervals for up to 90 min. Thereafter, a portion of the supernatant polymerization solution was filtered to remove from the supported catalyst under N_2 atmosphere into an empty reactor through a glass frit. The kinetics of the polymerization was then followed in both the solutions.

Figure 7a shows the first-order time-conversion plots for the polymerizations in the presence and absence of hydrated Na-clay supported catalyst. The polymerization in the presence of hydrated Na-clay supported catalyst progressed in a linear manner with a slight curvature at higher conversion. A downward curvature from the linearity in the first-order time−conversion plot is generally attributed to a decrease in active center concentration due to termination. The presence of termination would broaden the MWD of PBnMA. However, the PBnMAs obtained at higher conversions exhibited narrow MWD ($M_w/M_n \leq 1.30$), indicating the curvature could be attributed to an increase in viscosity, leading to the reduction in the rate of polymerization. On the other hand, the filtered solution without supported catalyst had a complete cessation of the polymerization from the time it was separated from the catalyst support (Figure 7a). As previously shown in batch polymerization, the UV−vis absorption of the filtered solution during the polymerization showed no absorbance at λ_{max} = 716 nm corresponding to the presence of $CuBr_2$/PMDETA, confirming the absence of catalyst in the solution (Figure 6-ii). Recently, Faucher and Zhu[44] showed such split-kinetics and confirmed the growth of polymer in the filtered solution as an indication for the presence of leached

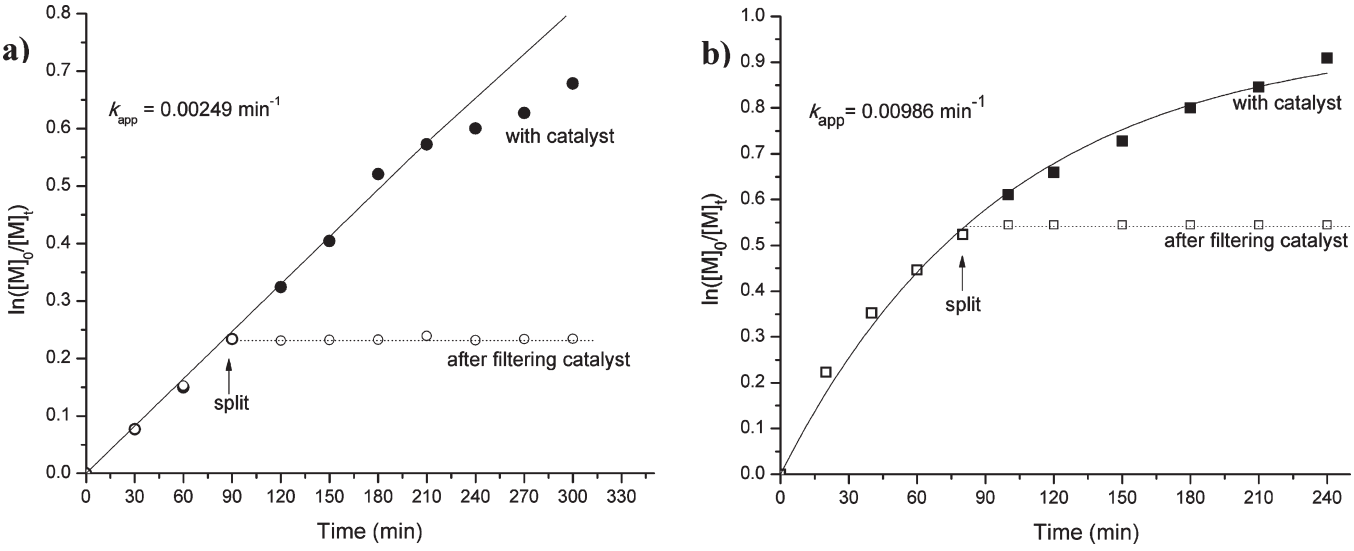

Figure 7. First-order time−conversion plots for the split-kinetics of (a) AGET ATRP of BnMA in anisole (1:1 v/v) at 40 °C in the presence and after separation from the hydrated Na-clay supported catalyst. Na-clay = 272 mg, Cu^{II}/Na-clay = 10 wt %, [BnMA] = 2.95 M, H_2O/Na-clay = 15 wt %, [EBriB] = 4.1 × 10^{-3} M, [NaAsc]/[I] = 0.17 and (b) ATRP of BnMA in anisole (1:1 v/v) at 25 °C in the presence and after separation from hydrated silica supported CuBr-PMDETA catalyst. Silica = 0.5 g, Cu^{I}/silica = 5 wt %, [BnMA] = 2.95 M, H_2O/silica = 20 wt %, [EBriB] = 7.5 × 10^{-3} M, BnMA/EBriB/Cu^{I}/PMDETA = 393/1/2/2 (Table 1, run 6).

catalyst in silica supported ATRP of MMA. The results of hydrated Na-clay system suggest that there is no catalyst present in the anisole, and the polymerization is occurring only at the hydrated surface.

Similarly, a split-kinetics investigation was performed to evaluate the behavior of BnMA polymerization using silica supported CuBr-PMDETA in the presence of water (H_2O/silica = 20 wt %). The rate of polymerization was fast, k_{app} = 0.009 86 min^{-1}, at the beginning but decreased gradually during the polymerization. The ln([M]$_0$/[M]$_t$) versus time plot showed a deviation from the linearity, indicating a decrease in the rate of the polymerization with increasing conversion (Figure 7b). Such a behavior was attributed to slow diffusion of chains approaching the support surface, due to high viscosity in the case of Na-clay supported catalyst system. However, the PBnMAs had broad MWD (∼1.8) irrespective of the conversion which suggests that the reaction proceeded with concurrent termination in the hydrated silica supported system. Thus, the deviation in the first-order time−conversion plot is attributed to the combination of termination and slow diffusion dynamics of the chains. The UV−vis spectrum of the filtered solution during the polymerization displayed no absorbance at λ_{max} = 716 nm. Once the solution was filtered from the hydrated silica, no further conversion was observed in the solution, indicating the absence of catalysts (Figure 7b).

The growth of PBnMA examined by SEC during the polymerization for both the supports showed a progressive increase in molecular weights and narrowing of MWD with increasing monomer conversion (Figures 8 and 9a). However, the molecular weights and MWDs of PBnMA aliquots taken at regular intervals after filtering from the catalyst solution remained nearly same and did not increase, confirming the absence of propagation in the filtered solution (Figures 8 and 9b). The absence of catalyst complexes in anisole and the absence of polymer growth in the filtered solution confirm that the polymerization is taking place on the surface of the hydrated regions in both the supports (clay and silica). The results further confirm that the hydration

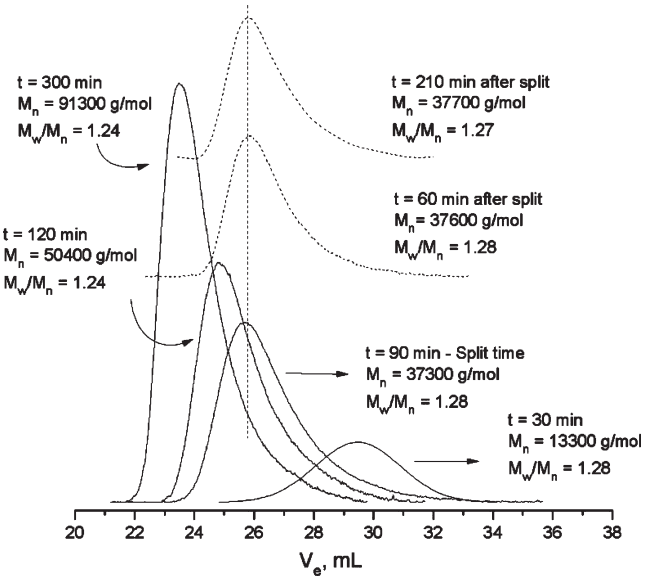

Figure 8. SEC traces of PBnMAs from split-kinetics of AGET ATRP in the presence of the hydrated Na-clay supported $CuBr_2$/PMDETA catalyst and after filtration of the hydrated Na-clay supported catalyst. Reaction conditions same as in Figure 7a.

helps in retaining the catalysts (Cu^{II} and Cu^{I}) localized on the surface of Na-clay and silica supports. The activation and deactivation occur only at the hydrated regions of the support independent of the nature of the supports.

Although both the supports retain the catalyst complexes on the surface with the help of hydration, they differ significantly in the deactivation efficiencies of the intermediate radicals at the interface. This can be observed via a comparative analysis of the MWDs of the PBnMAs in these supported catalyst systems. The obtained PBnMAs exhibited narrow MWD (M_w/M_n < 1.30) in

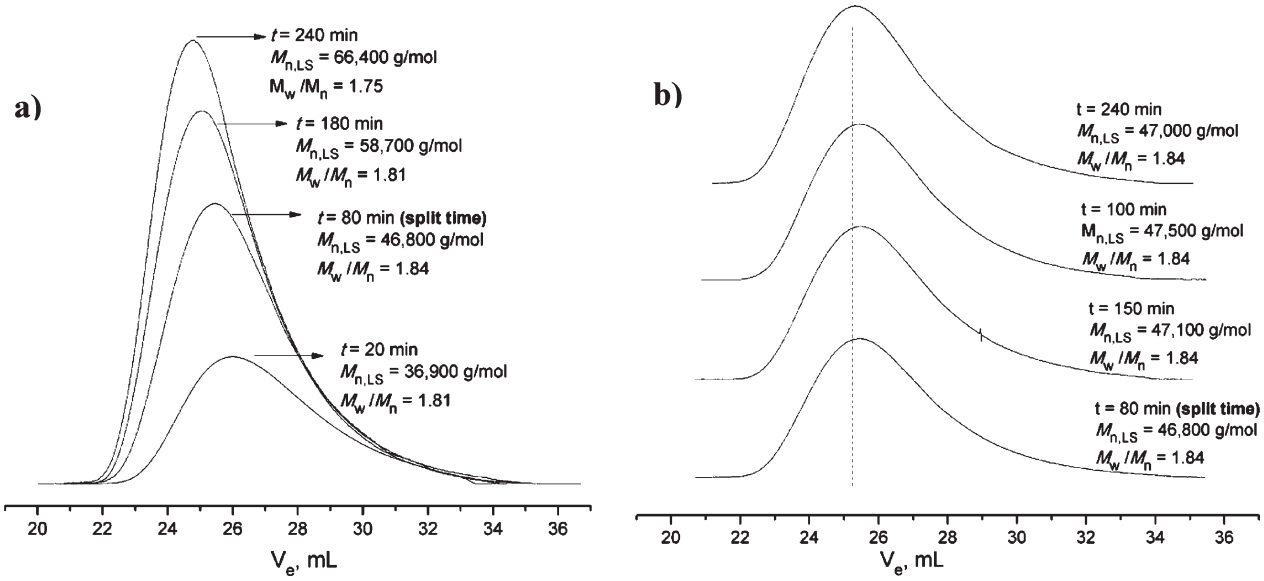

Figure 9. SEC traces of PBnMAs from split-kinetics of ATRP ATRP: (a) in the presence of the hydrated silica supported CuBr/PMDTEA catalyst and (b) after filtration of hydrated silica supported CuBr/PMDTEA catalyst. Polymerization conditions were same as in Figure 7b.

Table 2. Surface Area and Water Diffusivity Parameters of Different Inorganic Supports

support	surface area[a] (m^2/g)	particle size[b] (μm)	self-diffusion coeff[a,c] D_{water} (cm^2/s)	activation energy[d] $E_{D,water}$ (kJ mol^{-1})	refs
Na-clay	318−500	∼9−13	$\sim10^{-5}$	38−43	49−53
silica	550	∼40−63	$\sim10^{-12}-10^{-17}$	68−76	45−47, 54

[a] Values based on BET N_2 adsorption isotherm. [b] As per manufactures data-sheet. [c] Calculated using the BET equation. [d] Based on quasi-neutron elastic scattering.

the case of hydrated Na-clay system, which suggests that the deactivation of propagating radicals is rapid at the hydrated surface of the Na-clay. In contrary, the hydrated silica supported catalyst system produced PBnMAs with broad MWD (M_w/M_n > 1.52) right from the beginning. This distinct behavior is related to termination reactions at the hydrated interface; that the catalyst present at the hydrated silica surface is not efficiently available for the deactivation of growing radicals. This is supported from the plot of weight-average molecular weight vs conversion that showed a gradual increase confirming the presence of radical−radical coupling (Figure S1).

Critical Role of Water Diffusivity on the Support Surface. The availability of higher oxidation state catalyst complex in the vicinity of radicals at the interface is very important for a fast deactivation process. The lack of control in the polymerization is attributed to an inefficient deactivation which is related to the restricted mobility of the catalyst at the hydrated surface. As the catalyst is held on the surface of the support by water-hydrogen bonding, the diffusion of water plays an important role in the mobility of the catalyst. The obtained broad MWDs of the polymers suggest that the silica surface provides only a limited mobility for the catalyst. The limited accessibility of the catalyst on the hydrated surface can be attributed to a reported low self-diffusion coefficient ($D_{water} = 10^{-12}-10^{-17}$ cm^2/s) of water on the silica surface.[45−47] The self-diffusion coefficient of water on the silica surface is substantially lower than in the Na-clay surface and the bulk water ($D = 2.25 \times 10^{-5}$ cm^2/s) (Table 2).[48,49] This will decrease the mobility of the catalyst suspended in the hydrated layer and will reduce the deactivation rate of the growing radicals in silica supported catalyst system. Although, the average particle size of silica is much bigger than the clay in this study, the polymerization results are not influenced by the surface area as the nanosilica support also produced PBnMA with broad MWD (Table 1, run 7, Figure 4c).

Another factor associated with the slow diffusion of water on the silica surface is its high activation energy ($E_{D,water}$ = 68−76 kJ mol^{-1})[54] which is much higher than the $E_{D,water}$ for Na-clay (38−43 kJ mol^{-1}) as well as for bulk water (21 kJ/mol).[55] The high $E_{D,water}$ originates from strong hydrogen bonding between the surface hydroxyl groups and the adsorbed water molecules. According to high resolution ^1H NMR spectra, the water molecules are arranged in a tetrahedral fashion held together by strong hydrogen bonds with silica.[56] On the hydrated silica, water molecules are organized in multiple layers exhibiting a low entropy than that of the bulk water.[57,58] Reports have shown using inelastic neutron-scattering measurements that these layers constituting of double hydrogen-bonded water molecules are highly ordered and have negligible freedom of motion.[59] In fact, the differential scanning calorimetric studies of hydrated clay and hydrated silica with 30 wt % water showed that the desorption enthalpy of water from the silica surface is much higher ($\Delta H_{desorption}$ = 448 J/g) compared to the clay surface ($\Delta H_{desorption}$ = 305 J/g) (Figure 10). This further confirms that the water present on the silica is strongly held via hydrogen bonding.

Thus, the mobility of water on the silica surface is highly restricted, rendering an inefficient mobility for the suspended

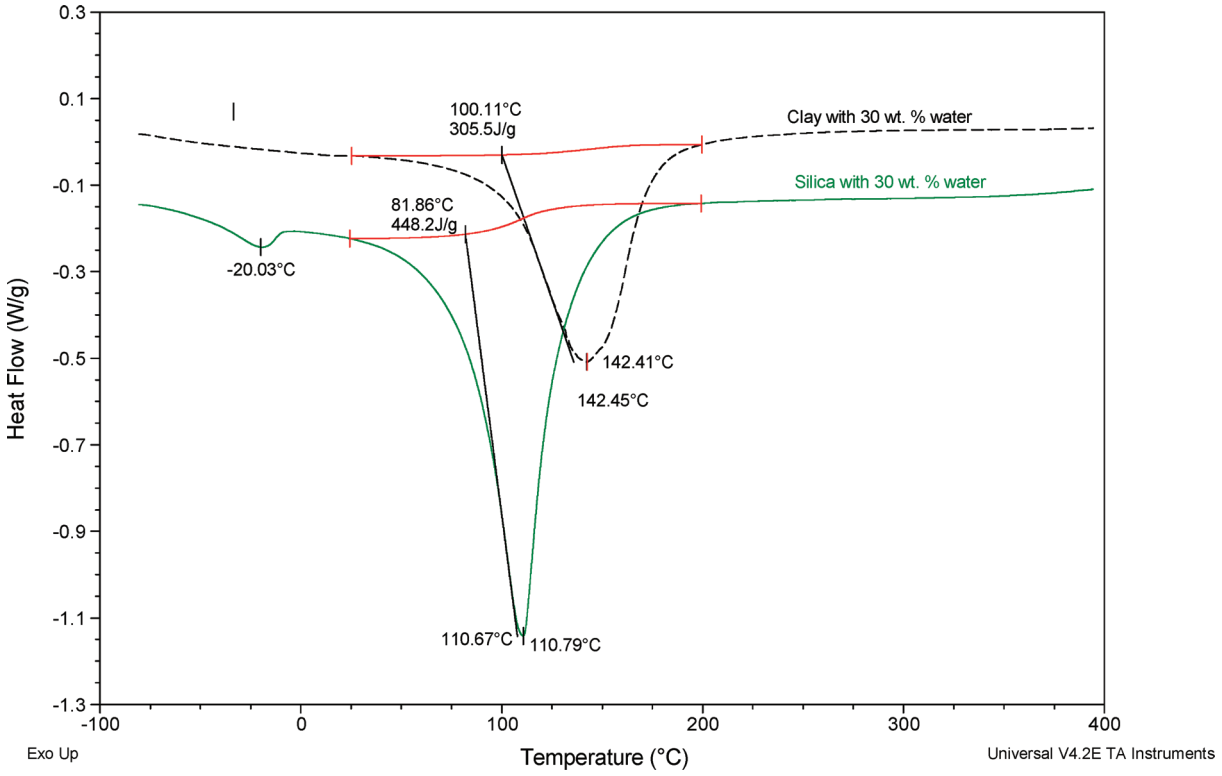

Figure 10. DSC endothermic peaks for desorption of water from clay and silica supports with 30 wt % hydration. Heating rate 10 °C/min.

Scheme 2. Arrangement of Water Molecules on the Surface of Silica and Aluminosilicate (Na-Clay): (a) Ordered Multilayer Hydration on the Surface of Silica; (b) Disordered Multilayer Hydration on the Surface of Aluminosilicate (Na-Clay)[a]

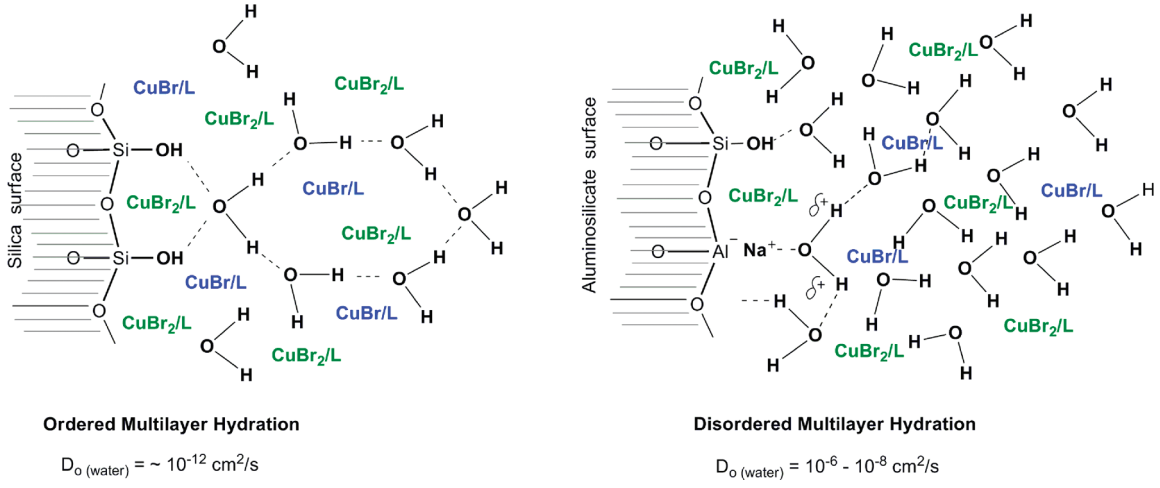

[a] The size of water molecules is exaggerated for a better pictorial understanding.

catalyst and thereby decreasing the deactivation rate of the propagating radicals (Scheme 2). The failure of hydration mediation in the silica supported catalysis for ATRP is solely attributed to strong/ordered (multilayer) hydrogen bonding with a very low water diffusion coefficient. In the case of hydrated Na-clay, the arrangement of water is disordered due to heterogeneous electron density on the surface from alternating aluminate and silicate bonds. Thus, the clay surface provides water molecules to exist in rapidly interchanging disordered (multilayer) hydrogen bonding. This is supported by the reported high diffusion coefficient of water on Na-clay ($D_{water} \sim 10^{-5}$ cm^2/s) which enhances free mobility of the suspended copper complexes. This favors a rapid deactivation of radical intermediates at the hydrated Na-clay interface, leading to polymers with narrow MWD in SAPC of ATRP. The results confirm that the propagation in SAPC ATRP is mediated by the hydration, but controlled by the dynamics of the water present at the surface of the support. The compartmentalization of propagation at the hydrated support surface can

Table 3. Kinetics of AGET ATRP of BnMA Using Hydrated Na-Clay Supported $CuBr_2$/PMDETA in the Presence of NaAsc in Anisole[a]

run	M/I/Cu^{II}/L[b] mole ratio	[I] × 10^3 (mol/L)	temp (°C)	conv[c] $x_{p,max}$	$M_{n,th}$[d] × 10^{-3} (g/mol)	$M_{n,SEC}$ × 10^{-3} [e] (g/mol)	$M_{n,LS}$ × 10^{-3} [f] (g/mol)	f[g]	M_w/M_n[e]	k_{app}[h] × 10^3 min^{-1}	$k_{app,avg}$[i] × 10^3 min^{-1}
1	894/1/2/2	3.3	40	0.49	77.5	91.2	142.3	0.54	1.24	2.76	2.69
2	720/1/2/2	4.1	40	0.53	67.8	84.0	131.0	0.52	1.26	2.51	2.46
3	536/1/2/2	5.5	40	0.55	51.7	63.5	99.1	0.52	1.26	2.79	2.82
4	536/1/2/2	5.5	20	0.28	26.2	40.1	62.6	0.42	1.32	1.04	-
5	536/1/2/2	5.5	60	0.66	62.2	73.1	114.0	0.55	1.28	5.42	-

[a] Reaction condition: Na-clay = 272 mg, Cu^{II}/clay = 10 wt %, H_2O/clay = 15 wt %, [NaAsc]/[I] = 0.17. [b] Cu^{II} = $CuBr_2$, L = PMDETA, I = EBriB, M = [BnMA] = 2.95 mol/L. [c] Conversion at t_{max}. [d] $M_{n,th}$ = (grams of monomer/mol of I) × x_p. [e] Determined by SEC using PS standards. [f] Determined using SEC-MALLS. [g] Initiator efficiency, $f = M_{n,th}/M_{n,LS}$. [h] Apparent rate constant, k_{app}, determined from the initial slope of the first-order time−conversion plots. [i] $k_{app\text{-}avg}$ calculated by taking average of slopes taken at 2, 3, and 4 h.

be verified through the determination of reaction order as the surface containment of heterogeneous reactions would follow zero-order kinetics.

Determination of Reaction Order for Clay Supported AGET ATRP. The kinetics of heterogeneous hydrated Na-clay supported polymerization of BnMA was investigated in order to understand the mechanistic aspects of the system. Accordingly, AGET ATRP of BnMA (2.95 M) using Na-clay (272 mg) supported with 10 wt % $CuBr_2$/PMDETA in the presence of 15 wt % H_2O relative to the support was performed at different concentrations of the initiator (EBriB) in anisole (1:1 v/v) at 40 °C (Table 3). The concentration of NaAsc was kept constant for all the reactions ([NaAsc]/[I] = 0.17). Since an excess amount of $CuBr_2$/L was used on the support, the kinetics was analyzed using Matyjaszewski's equation as given below:[60]

$$\ln \frac{[M]_0}{[M]_t} = k_p K_{eq} \frac{[RX][Cu^I]}{[Cu^{II}]} t = k_{app} t \quad (1)$$

The first-order time−conversion plots showed a linear monomer conversion for up to 180 min and then slightly deviated at later stages of the polymerization. The deviation at higher conversion is not related to termination but attributed to high viscosity of the heterogeneous polymerization medium as described earlier (Figure 11a). A slight acceleration of the rate is noticeable at ~300 min, which could result from a slow diffusion of active chains at the expanded intercalary regions exposed in the hydrated clay. Hence, the apparent rate constant, k_{app}, was determined from the initial slope. An average value of the slope, $k_{app,avg}$, was also calculated using three different maximum polymerization times (2, 3, and 4 h) to minimize the error associated with the initial slope determination. Interestingly, both k_{app} and $k_{app,avg}$ values were similar, and more importantly, they indicated that the rate of the polymerization was independent of the initiator concentration (Table 3). The bilogarithmic plot $k_{app,avg}$ vs [I] showed a slope of 0.0045 ± 0.11, indicating the polymerization follows a zero-order kinetic with respect to the bulk initiator concentration in anisole (Figure 11b). The reaction order plot using k_{app} also gave a slope of 0.04 ± 0.20 (Figure S2 in Supporting Information).

Thus, in SAPC of ATRP, a minute concentration of the initiator that is present at the hydrated interface of Na-clay determines the apparent rate of the polymerization independent of the bulk initiator concentration available in anisole. This is in contrast with the usual first-order rate dependence on the initiator concentration reported for conventional ATRP as well as solid supported catalyst systems.[25,29,33,34,36,61]

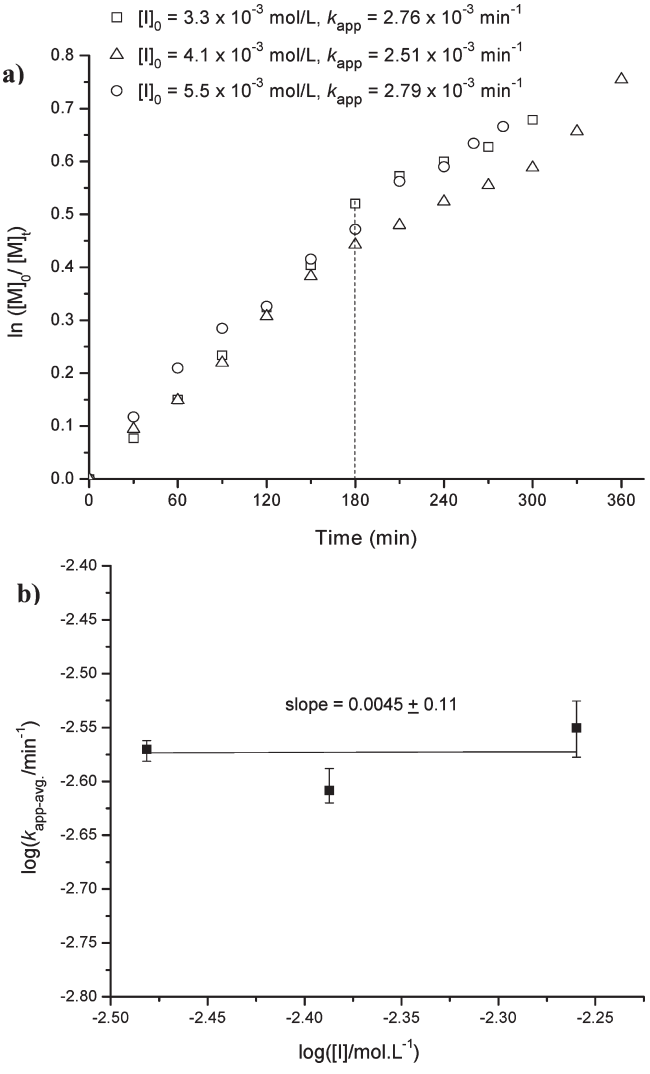

Figure 11. (a) First-order time−conversion plots for AGET ATRP of BnMA using hydrated Na-clay supported $CuBr_2$/PMDETA with different initiator concentrations. Na-clay = 272 mg, Cu^{II}/clay = 10 wt %, [BnMA] = 2.95 M, H_2O/clay = 15 wt %, [NaAsc]/[I] = 0.17. (b) Bilogarithmic plot of $k_{app\text{-}avg}$ versus initiator concentration.

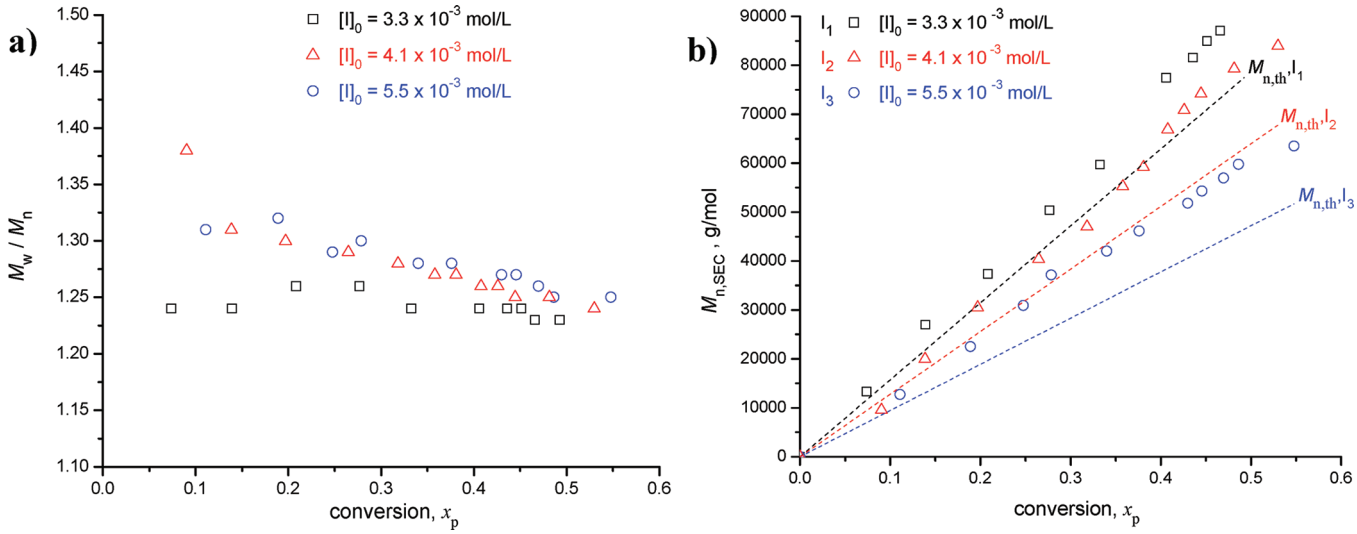

Figure 12. (a) Molecular weight distribution as a function of conversion for AGET ATRPs of BnMA using hydrated Na-clay supported $CuBr_2$/PMDETA with different initiator concentrations. (b) Molecular weight ($M_{n,SEC}$) as a function of conversion in the AGET ATRP of BnMA using hydrated Na-clay supported $CuBr_2$/PMDETA with different concentrations of initiator in anisole at 40 °C (Table 2). $M_{n,SEC}$ based on PS standards. Reaction conditions same as in Figure 10.

The zero-order reaction is an indication of a true heterogeneous nature of the polymerization and supports that the propagation is contained at the hydrated interface of Na-clay. Unlike other reported covalent and noncovalent supported catalyst systems wherein the polymerization proceeds simultaneously at the surface as well as in the organic phase due to strong partitioning or leaching of the immobilized catalyst,[36] the propagation in the Na-clay supported catalyst system is mediated by the hydration and compartmentalized within the hydrated layers of the support surface.

The supported catalyst system for ATRP using hydrated Na-clay is the first one to exhibit zero-order kinetics confirming that an entire redox equilibrium polymerization is contained at the surface. An easy availability of both the Cu^{II} and Cu^{I} complexes on the surface is essential for a fast deactivation of intermediate radicals. This is provided by the high diffusion of water at the hydrated clay surface to produce moderately narrow molecular weight distributed polymers. In fact, the PBnMAs obtained at regular internal showed a narrowing of MWD with increasing conversion and a linear increase of $M_{n,SEC}$ with conversion also conforming absence of transfer reaction (Figure 12).

Effect of Temperature. The effect of temperature on the rate of polymerization was studied in the temperature range from 20 to 60 °C (Table 2, runs 3−5). The k_{app} determined from the initial slope of the first-order time−conversion plots increased with increasing temperature (Figure 13). The kinetic plots of AGET ATRP displayed a deviation at higher conversion owing to the viscosity phenomenon as was seen in the reactions at different concentrations of the initiator. The k_{app} decreased slightly between 120 and 240 min depending on the reaction temperature followed by an acceleration of the rate. As previously discussed, the curvature is not suggestive of the termination as the PBnMAs obtained at higher conversions exhibit narrow MWDs (Figure S3, Supporting Information).

The Arrhenius plot, $\ln(k_{app})$ vs $(1/T)$, for the polymerization of BnMA using the Na-clay supported ATRP system is presented in Figure 14. Based on the slope, the apparent activation energy ($\Delta E^{\neq}_{app}$) was calculated as 33.5 ± 2.2 kJ mol^{-1}, which is quite a

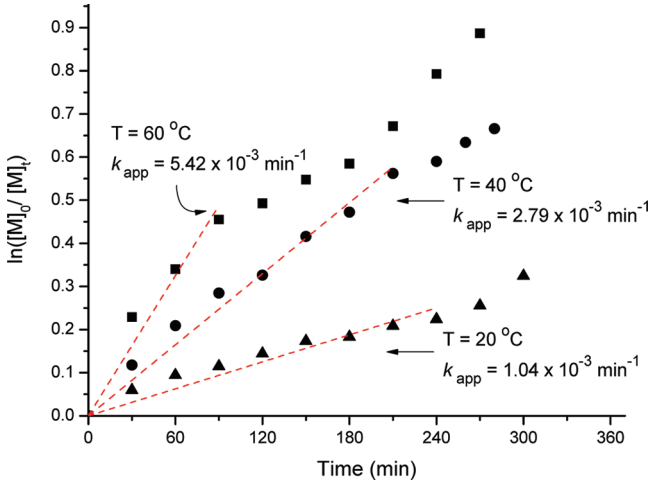

Figure 13. First-order time−conversion plots for AGET ATRP of BnMA in anisole (1:1 v/v) using Na-clay loaded with 10 wt % $CuBr_2$−PMDETA catalyst at different temperatures: Na-clay catalyst = 272 mg; [BnMA] = 2.95 mol/L; $[I]_0 = 5.5 \times 10^{-3}$ M: 20 °C (▲; Table 2, run 4), 40 °C (●; Table 2, run 3), 60 °C (■; Table 2, run 5).

low value than the values of apparent activation energy reported for conventional ATRPs of MMA, methyl acrylate, and n-butyl acrylate.[34,58,62] More importantly, the pre-exponential factor was found to be very low, ln A = 2.85 ± 0.88, much smaller than for the homogeneous ATRP.[63] A known activation energy of the propagation ($\Delta E^{\neq}_{p}$) for MMA (22.2 kJ mol^{-1})[63] was used to calculate an apparent enthalpy of the ATRP equilibrium (ΔH°_{app}) according to the equation

$$\Delta H^{\circ}_{app} = \Delta E^{\neq}_{app} - \Delta E^{\neq}_{prop} \quad (2)$$

The estimated enthalpy of the equilibrium was 11.3 kJ mol^{-1} for the Na-clay surface contained SAPC ATRP. This is quite lower than the literature value reported for the homogeneous solution polymerization of MMA (40.6 kJ mol^{-1}).[63] Although

dx.doi.org/10.1021/ma201961e |Macromolecules 2011, 44, 8805–8818

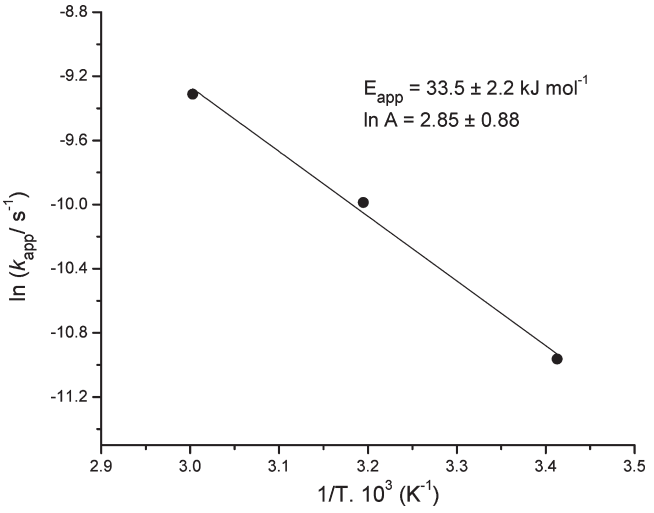

Figure 14. Arrhenius plot of ln k_{app} vs $(1/T)$ of AGET ATRP of BnMA at different temperatures. Reactions conditions were the same as in Figure 13.

the polymerization proceeds at the surface of the hydrated clay, a huge intercalary expansion in the presence of water (H_2O/clay ~17 wt %) would provide considerable interface area from the expanded intercalaries and their exposed edges for the polymerization. Activation and deactivation of chains at the edge regions are confined in between the clay layers. These lower values could be attributed to the effect of confined propagation at the intercalary layers of hydrated clay support.

The steady-state concentration of the propagating radicals can be estimated from the eq 3.

$$k_{app}[M] = k_p[P^\bullet][M] \quad (3)$$

The reported rate constant of radical propagation for MMA of ($k_p = 1.616 \times 10^3$ M^{-1} s^{-1} at 90 °C) was combined with the values of k_{app} to obtain the concentration of radicals during the polymerization according to eq 4.

$$[P^\bullet] = \frac{k_{app}}{k_p} \quad (4)$$

The obtained radical concentrations for different initiator concentrations are listed in Table 3. Since it is a zero-order reaction with respect to initiator concentration and the k_{app} values are nearly same, the steady-state concentration of radicals generated during the polymerization was found to be constant (~2.8×10^{-8} mol/L) irrespective of the initiator concentration (Table 3). The K_{eq} for conventional ATRP systems is usually determined from the steady-state concentration of radicals using the equation

$$K_{eq} = \frac{[P^\bullet][Cu^{II}X_2]}{[Cu^{I}X][RX]} \quad (5)$$

In typical ATRP systems the concentration of radicals generated during the polymerization and k_{app} are proportional to the amount of initiator used; hence, those terms are required in the estimation of K_{eq}. However, the rate of hydrated Na-clay supported polymerization presented here follows a zero-order dependence on the initiator concentration ([RX]). Hence, the k_{app}, and $[P^\bullet]$ are independent of the $[RX]_0$ (Table 4).

The concentration of active radicals and RX at the interface remain same in all the polymerizations, and thus, K_{eq} can be

Table 4. Steady-State Concentration of Radicals for AGET ATRP of BnMA in Anisole Using Hydrated Na-Clay Supported Catalysts at Different Initiator Concentrations at 40 °C

[I] (mol/L)	k_{app}[a] × 10^5 s^{-1}	$[P^\bullet] = k_{app}/k_p$[b] × 10^8 (mol/L)	$[Cu^{II}]_0/[Cu^{I}]_0 = K_{eq}/\alpha$[c]
3.3	4.60	2.85	10
4.1	4.18	2.59	10
5.5	4.65	2.88	10

[a] k_{app} was calculated using initial slopes of the plot. [b] k_p of 1.616×10^3 M^{-1} s^{-1} was used for the calculation. [c] α is a constant, $[P^\bullet]/[RX]_0$ at the interface and $[Cu^{I}]_0 = [NaAcs]_0$.

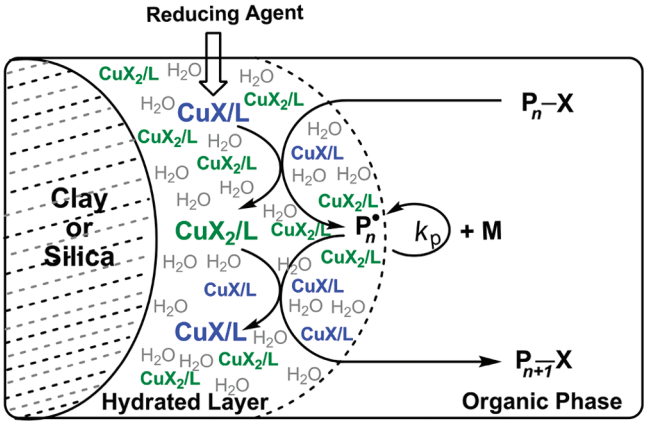

Figure 15. Mechanism of the hydrated Na-clay supported $CuBr_2$/L catalyst system for AGET ATRP. The size of hydrated layer in the illustration is exaggerated for visualization purposes.

given by eq 6:

$$K_{eq} = \alpha\frac{[Cu^{II}X_2]}{[Cu^{I}X]} \quad \text{where } \alpha = \frac{[P^\bullet]}{[RX]} \quad (6)$$

Therefore, as long as the ratio of Cu^{II}/Cu^{I} is maintained on the support for a fixed amount of clay and hydration, the value of K_{eq} should remain same irrespective of the $[I]_0$. This is a unique behavior observed for this truly supported ATRP catalyst system involving equilibrium activation and deactivation processes at the surface.

Proposed Mechanism. The catalyst containment at the hydrated layers of the supported surface and its easy accessibility for a fast deactivation process can be explained on the basis of low partitioning of the catalyst complexes and their enhanced mobility over the hydrated surface of the support. Figure 15 depicts the proposed mechanism for the supported aqueous-phase catalysis for ATRP. The interaction of initiating species (EBriB) present in the bulk organic solution with $Cu^{I}Br$/L on the hydrated support generates radicals at the hydrated interface for initiation of monomer that diffuses into the interface. Upon initiation, the propagating radicals are rapidly deactivated by a large amount of $Cu^{II}Br_2$/L readily available at the interface before diffusing out to the organic solution.

The hydration provides a low partitioning for the catalyst on the support and enables deactivated-dormant polymer chains diffuse to the bulk organic solvent. This establishes a contact equilibrium between the hydrated surface of the support and the dormant polymer chain in the organic solution. Several factors can affect

this equilibrium such as the polarity of organic phase and the diffusion characteristics of the halogen terminated dormant polymer chain in the solution.[42] Surface structure also places a significant role in determining the efficiency of this equilibrium. In the case of hydrated clay, the polymer chains that interact with the edge regions of expanded intercalary have an effect of a confinement that can either decrease or increase the rate of the activation/deactivation depending on the size of the interacting polymer chain.

At high conversions, the viscosity of the heterogeneous polymerization solution becomes high, which would decrease the rate of diffusion of dormant chains to the surface and reduce the reaction rate. The rate enhancement due to limited radical diffusion leading to Trommsdorf effect as in the case of classical radical polymerization would not occur in the hydration mediated supported ATRP because only dormant chains are present in the organic phase. As a result, the propagation reaction is restricted to the hydrated interface of the support, and no polymerization occurs in the bulk organic layer of the heterogeneous reaction medium. This unique hydration mediated SAPC for ATRP can be performed in a flow-through reactor to 100% monomer conversion without a significant increase in the viscosity of the polymerization solution.

CONCLUSIONS

The supported aqueous phase catalysis using hydrated Na-clay and silica supports for ATRP of BnMA and MMA in anisole has been studied at 25 and 60 °C, respectively, using batch and kinetics experiments. The polymerization in the presence of a small amount of water on these supports for ATRP and AGET ATRP using CuBr-L and $CuBr_2$-L, respectively, showed that the adsorbed catalyst complexes are totally retained on the surface, and no leaching is observed into the anisole. The polymerization of BnMA proceeded in a living manner and PBnMAs of narrow MWD ($M_w/M_n < 1.3$) were obtained using hydrated Na-clay catalyst support whereas the polymers obtained from the hydrated silica catalyst support produced broad MWD ($M_w/M_n > 1.5$). Unique hydrogen bonding with a very low diffusion coefficient of water was attributed to inefficient deactivation of intermediate radicals due to slow mobility of the suspended catalyst in the hydrated silica support. The polymerization of BnMA was found to follow zero reaction order with respect to initiator concentration in hydrated Na-clay supported catalyst system (H_2O/Na-clay $\approx$ 17 wt %) in the presence of sodium ascorbate ($0.15 \leq [NaAsc]_0/[I]_0 \leq 0.23$). The polymerization rate increased with the reaction temperature, and an apparent activation energy, $E_{app}^{\neq}$, and pre-exponential factor were calculated as 33.5 kJ/mol and 17.3 ($\ln A = 2.85$), respectively. The calculated $\Delta H_{app}^{\circ} = 11.3$ kJ/mol for the polymerization of BnMA using Na-clay supported ATRP, on the basis of the reported activation of energy for the propagation of MMA, was quite lower than the reported values for MMA polymerization in conventional ATRP systems. The results showed that the hydration is the key in compartmentalizing the propagation at the surface and played an important role in promoting activation/deactivation processes at a thin aqueous interface between the support and the organic phase thus controlling the polymerization.

Thus, the SAPC is effective in hydrated Na-clay, which has high diffusion coefficient and low diffusion activation energy for water compared to silica gel. This is because of the nonuniform and disordered layers of weakly hydrogen-bonded water molecules enabling suspended catalyst complexes to move freely over the surface for a rapid deactivation of intermediate radicals.

ASSOCIATED CONTENT

Supporting Information. A plot of molecular weight determined by light scattering ($M_{n,LS}$) and molecular weight distribution (M_w/M_n) vs conversion for split kinetic experiment of BnMA polymerization using hydrated silica support, a plot of k_{app} vs $[I]_0$, and plots of $M_{n,LS}$ and M_w/M_n vs conversion for the AGET ATRP of BnMA in the presence of hydrated Na-clay. This material is available free of charge via the Internet at http://pubs.acs.org.

AUTHOR INFORMATION

Corresponding Author

*E-mail: baskaran@utk.edu. Phone: 865-974-5583.

Present Address

[†]Exxon Mobil, 5200 Bayway Drive, Baytown, TX 77522.

ACKNOWLEDGMENT

Financial support for this project by the US Department of Energy, DOE (DE-AC05-00OR22725), is graciously acknowledged. D.B. thanks one of the reviewers of this manuscript, who inspired to add a valuable argument in the Introduction.

REFERENCES

(1) Wang, J.-S.; Matyjaszewski, K. *J. Am. Chem. Soc.* **1995**, *117* (20), 5614–5614.
(2) Kato, M.; Kamigaito, M.; Sawamoto, M.; Higashimura, T. *Macromolecules* **1995**, *28*, 1721–1723.
(3) Percec, V.; Barboiu, B. *Macromolecules* **1995**, *28* (23), 7970–7972.
(4) Matyjaszewski, K.; Xia, J. *Chem. Rev.* **2001**, *101*, 2921–2990.
(5) Kamigaito, M.; Ando, T.; Sawamoto, M. *Chem. Rev.* **2001**, *101*, 3689–3745.
(6) Wakioka, M.; Baek, K. Y.; Ando, T.; Kamigaito, M.; Sawamoto, M. *Macromolecules* **2002**, *35*, 330.
(7) Uegaki, H.; Kotani, Y.; Kamigaito, M.; Sawamoto, M. *Macromolecules* **1997**, *30* (8), 2249–2253.
(8) Matyjaszewski, K.; Coca, S.; Gaynor, S. G.; Wei, M.; Woodworth, B. E. *Macromolecules* **1997**, *30* (23), 7348–7350.
(9) Percec, V.; Guliashvili, T.; Ladislaw, J. S.; Wistrand, A.; Stjerndahl, A.; Sienkowska, M. J.; Monteiro, M. J.; Sahoo, S. *J. Am. Chem. Soc.* **2006**, *128* (43), 14156–14165.
(10) Shen, Y.; Tang, H.; Ding, S. *Prog. Polym. Sci.* **2004**, *29*, 1053–1078.
(11) Honigfort, M. E.; Brittain, W. J.; Bosanac, T.; Wilcox, C. S. *Macromolecules* **2002**, *35*, 4849–4851.
(12) Sarbu, T.; Matyjaszewski, K. *Macromol. Chem. Phys.* **2001**, *202* (17), 3379–3391.
(13) Ding, S.; Yang, J.; Radosz, M.; Shen, Y. *J. Polym. Sci., Part A: Polym. Chem.* **2004**, *42* (1), 22–30.
(14) Shen, Y.; Zhu, S.; Pelton, R. *Macromolecules* **2001**, *34*, 3182–3185.
(15) Tsarevsky, N. V.; Matyjaszewski, K. *Chem. Rev.* **2007**, *107*, 2270–2299.
(16) Honigfort, M. E.; Brittain, W. J. *Macromolecules* **2003**, *36*, 3111–3114.
(17) Matyjaszewski, K.; Pintauer, T.; Gaynor, S. *Macromolecules* **2000**, *33*, 1476–1478.
(18) Matyjaszewski, K.; Jakubowski, W.; Min, K.; Tang, W.; Huang, J.; Braunecker, W. A.; Tsarevsky, N. V. *Proc. Natl. Acad. Sci. U. S. A.* **2006**, *103* (42), 15309–15314.
(19) Xia, J.; Matyjaszewski, K. *Macromolecules* **1997**, *30*, 7697.

(20) Jakubowski, W.; Min, K.; Matyjaszewski, K. *Macromolecules* **2005**, *39* (1), 39–45.
(21) Jakubowski, W.; Matyjaszewski, K. *Macromolecules* **2005**, *38* (10), 4139–4146.
(22) Min, K.; Gao, H.; Matyjaszewski, K. *J. Am. Chem. Soc.* **2005**, *127* (11), 3825–3830.
(23) Xia, J.; Matyjaszewski, K. *Macromolecules* **1997**, *30* (25), 7692.
(24) Faucher, S.; Zhu, S. *Ind. Eng. Chem. Res.* **2005**, *44*, 677.
(25) Kickelbick, G.; Paik, H. J.; Matyjaszewski, K. *Macromolecules* **1999**, *32* (9), 2941–2947.
(26) Hong, S. C.; Paik, H.-J.; Matyjaszewski, K. *Macromolecules* **2001**, *34*, 5099–5102.
(27) Haddleton, D. M.; Kukulj, D.; Radigue, A. P. *Chem. Commun.* **1999**, 99–101.
(28) Noda, T.; Grice, A. J.; Levere, M. E.; Haddleton, D. M. *Eur. Polym. J.* **2007**, *43*, 2321–2330.
(29) Nguyen, J. V.; Jones, C. W. *Macromolecules* **2004**, *37* (4), 1190–1203.
(30) Faucher, S.; Zhu, S. *J. Polym. Sci., Part A: Polym. Chem.* **2007**, *45*, 553–565.
(31) Shen, Y.; Zhu, S.; Zeng, F.; Pelton, R. H. *Macromolecules* **2000**, *33* (15), 5427–5431.
(32) Hong, S. C.; Matyjaszewski, K. *Macromolecules* **2002**, *35*, 7592–7605.
(33) Haddleton, D. M.; Duncalf, D. J.; Kukuli, D.; Radigue, A. P. *Macromolecules* **1999**, *32*, 4769–4775.
(34) Shen, Y.; Zhu, S.; Zeng, F.; Pelton, R. *J. Polym. Sci., Part A: Polym. Chem.* **2001**, *39* (7), 1051–1059.
(35) Faucher, S.; Zhu, S. *Macromolecules* **2006**, *39*, 4690–4695.
(36) Faucher, S.; Zhu, S. *Macromol. Rapid Commun.* **2004**, *25*, 991–994.
(37) Haddleton, D. M.; Jackson, S. G.; Bon, S. A. F. *J. Am. Chem. Soc.* **2000**, *122* (7), 1542–1543.
(38) Shen, Y.; Zhu, S. *Macromolecules* **2001**, *34* (25), 8603–8609.
(39) Munirasu, S.; Aggarwal, R.; Baskaran, D. *Chem. Commun.* **2009**, 4518–4520.
(40) Baskaran, D.; Munirasu, S. A process for the development of recyclable and reversible clay catalyst for metal mediated polymerization. Indian Patent Application # 1712DEL2007, 10th Aug, 2007.
(41) Munirasu, S.; Deshpande, A.; Baskaran, D. *Macromol. Rapid Commun.* **2008**, *29*, 1538–1543.
(42) Aggarwal, R.; Baskaran, D. *J. Polym. Sci., Part A: Polym. Chem.* **2011**, DOI: 10.1002/pola.24968.
(43) Nguyen, J. V.; Jones, C. W. *Macromolecules* **2004**, *37* (4), 1190–1203.
(44) Faucher, S.; Zhu, S. *Macromol. Rapid Commun.* **2004**, *25* (10), 991–994.
(45) Thurn, J. *J. Non-Cryst. Solids* **2008**, *354*, 5459.
(46) Iler, R. K. *The Chemistry of Silica*; John Wiley and Sons: New York, 1978.
(47) Paprier, E. *Adsorption on Silica Surfaces*; Marcel Dekker: New York, 2000.
(48) Gillen, K. T.; Douglas, D. C.; Hoch, M. J. R. *J. Chem. Phys.* **1972**, *57*, 5117.
(49) Trappeniers, N. J.; Gerritsma, P. H.; Oosting, P. H. *Phys. Rev. Lett.* **1965**, *18*, 256.
(50) Thomas, J.; Bohor, B. F. *Clays Clay Miner.* **1968**, *16*, 83.
(51) Juang, R.-S.; Lin, S.-H.; Huang, F.-S.; Cheng, C.-H. *J. Colloid Interface Sci.* **2004**, *274*, 337.
(52) Gonzalez, F.; Juranyi, F.; Van Loon, L.; Gimmi, T. *Eur. Phys. J. Spec. Top.* **2007**, *141*, 65–68.
(53) Zabat, M.; Van Damme, H. *Clay Minerals* **2000**, *35*, 357.
(54) Palandari, J. L.; Kharaka, Y. K. A compilation of rate parameters of water-mineral interaction kinetics for application to geochemical modeling, U.S. Department of Geological Survey, 2004.
(55) Parravano, C.; Baldeschwieler, J. D.; Boudart, M. *Science* **1967**, *155*, 1535.
(56) Avedikian, L. *Bull. Soc. Chim.* **1971**, 2832.
(57) Overloop, K.; Van Gerven, L. *J. Magn. Reson., Ser. A* **1993**, *101*, 147.
(58) Sermon, P. A. *J. Chem. Soc., Faraday Trans. 1* **1980**, *76*, 885.
(59) Hall, P. G.; Pidduck, A.; Wright, C. J. *J. Colloid Interface Sci.* **1981**, *79*, 339.
(60) Matyjaszewski, K.; Patten, T. E.; Xia, J. *J. Am. Chem. Soc.* **1997**, *119* (4), 674–680.
(61) Goto, A.; Fukuda, T. *Prog. Polym. Sci.* **2004**, *29* (4), 329–385.
(62) Davis, K. A.; Paik, H.-j.; Matyjaszewski, K. *Macromolecules* **1999**, *32*, 1767.
(63) Wang, J.-L.; Grimaud, T.; Matyjaszewski, K. *Macromolecules* **1997**, *30* (21), 6507–6512.